SUPPLEMENTAL MATERIAL:

Supplemental Methods:

Cell culture: PASMC (less than passage 6) were grown in high-glucose DMEM supplemented with 10% FBS (Gibco, Invitrogen, Burlington, ON, Canada) and 1% antibiotic/antimytotic (Gibco, Invitrogen, Burlington, ON, Canada)[1].

Cell treatments: All treatments from EMD Bioscience, (Mississaga, ON, CANADA) were diluted in DMSO (DMSO final concentration <0.001%). Endothelin 1 (10nM), Angiotensin 2 (200nM), PDGF (30ng.mL^{-1}), TNFα (100ng.mL^{-1}) and Quercetagetine (1μM) were applied for 48h. siRNA (from AMBION, Austin, TX, USA) were transfected at a final concentration of 20nM with $CaCl_2$. After 12h, medium was changed and experiments were performed 48h after the beginning of the transfection. Adenoviruses were used by simply infection (1×10^7PFU) for 48h as previously described [1, 2]. Efficiencies of siRNA transfections and adenoviruses infections rates were assessed in Supplemental Fig.11.

Measurement of the $\Delta\Psi m$ and $[Ca^{2+}]_i$ in live PASMCs (37°C) were performed using tetramethylrhodamine methyl-ester perchlorate (TMRM) and Fluo-3AM from Invitrogen (Branchburg, NJ, USA) at a final concentration of 5μM, as previously described[3, 4].

Proliferation and apoptosis measurements: To study the effect of STAT3 and Pim1 on PASMC proliferation and apoptosis *in vitro*, we established a model where cultured human PAH-PASMCs were exposed to 10% FBS (a condition that is known to promote proliferation)[1, 4] or 0.1% FBS (a "starvation" condition that promotes apoptosis)[1, 4]. PASMC apoptosis and proliferation were measured using Apoptag apoptosis detection kit (TUNEL; Millipore, Temecula, CA) and the proliferating cell nuclear antigen PCNA antibody from (DAKO, Carpinteria, CA) according to the manufacturer's instructions[3, 4]. Percent of nuclei positive PASMCs for TUNEL or PCNA were determined.

Nuclear translocation assay: nuclear localization was measured by immunofluorescence. In humans/rats and mice lungs biopsies PAs were previously stained with SM-Actin (Sigma, 1/5000), STAT3 and NFATc2 activation were measured only in SM-Actin

positive cells within distal PAs (<1500µm in human, <400µm in rats and <300µm in mice) in at least 5 to 10 PAs per patient/rat/mice at least in 5 patients/rats/mice. In PASMCs, STAT3 and NFATc2 activation were measured in at least 50 PASMCs per experiment per patient. At least 3 experiments were performed in 3 PAH and 5 healthy patients. Briefly, PY705-STAT3 (Cell Signaling, 1/250) and NFATc2 (ABCam, 1/250) staining were performed as previously described[4]. Secondary antibodies used were Alexa Fluor 488 or 594 (Invitrogen, Branchburg, NJ, USA). Co-localization between the targeted protein stained in red or green and the nucleus stained in blue with DAPI was assessed using Volocity software from Perkin Elmer USA. Co-localization was assessed at least in 5 to 10 distal arteries (<1500µm in human, <400µm in rats and <300µm in mice) per patient/rat/mice at least in 5 patients/rats/mice. Number of positive cells (with clear co-localization between target and DAPI) was measured. Positive PASMCs/total number of cells ratio was quantified and presented as the percentage of target activation.

NFAT luciferase assay: Cells were plated in 24-well plate, with 1×10^5 cells per well. NFAT luciferase adenovirus was transfected at 1×10^7PFU. After 12h, medium was changed and treatments were applied for 48h. Cells were lysed, and luminescence was detected using the Luciferase Assay System (Promega) according to the manufacturer's instructions. Luminescence counts were standardized to protein content.

Quantitative RT-PCR and immunoblots were performed as previously described[3,4] qRT-PCR $2^{\Delta\Delta Ct}$ were calculated with 18s as housekeeping gene (Taqman Gene expression Assay, Applied Biosystem, Foster, CA, USA). For immunoblots, protein expression of PY705-STAT3, STAT3, PS473-Akt, Akt, PY701-STAT1, STAT1, PY694-STAT5, STAT5, PS112-Bad, Bad, NFATc2 were quantified and normalized to both smooth muscle actin (Santa Cruz Biotechnology, 1/500) and Amido Black as previously described[4]. PY705-STAT3/STAT3, PS473-Akt/Akt, PY701-STAT1/STAT1, PY694-STAT5/STAT5 and PS112-Bad/Bad ratios evaluation were obtained from the same gel after 30min stripping at 50 degrees.

In vivo experiments: Rats were injected s.c. with 60mg.Kg^{-1} of MCT. Mice were injected i.v. with 5mg.Kg^{-1} of monocrotaline pyrrole (MCTP) as previously described[5]. Monocrotaline was converted to MCTP using the methodology of Mattocks *et al*[6]. Intra-tracheal nebulization was given on day 18, siSCR (AMBION, 1nmol) and siPim1 (AMBION, 1nmol) were combined with Invivofectamine (Invitrogen, Canada) as described by manufacturer. Mice CH were placed for 2 weeks in normobaric hypoxic chambers maintained with 5.5 l min^{-1} flow of hypoxic air (10% O_2 and 90% N_2). Chambers were opened twice a week for cleaning and replenishment of food and water. Oxygen concentrations were continuously monitored with blood gas analyzers. Soda lime was used to lower carbon dioxide concentration.

Hemodynamic measurements: All rats and mice underwent hemodynamic and echocardiography (vevo 2100 visualsonics) studies as previously described[4] [7]. Right catheterizations (closed chest) were performed using SciScence catheters. Direct PA pressures were measured in both rats and mice.

Histology measurements: % media wall thickness was assessed in distal PAs in rats (<400μm) and mice (<300μm) as previously described[4], at least in 5 to 10 distal arteries per rats/mice in least in 5 rats/mice were considered.

ChIP-PCR. The binding of STAT3 on 3' region of Pim1 gene was studied in ET-1 stimulated PASMCs from 3 control patients. The activation of STAT3 by ET-1 was confirmed by immunoblots as shown in (Fig.1). Cross-links were generated with 1% formaldehyde and chromatin was extracted in lysis buffer (50mM Tris-HCl pH8; 10mM EDTA; 0,2 % SDS and 5mM Na-Butyrate). Chromatin was then sheared by sonication (Diagenode Bioruptor) on ice to an average length of 750bp. After pre-clearing with a mix of protein A/G sepharose beads (4°C for 1 hour), 80μg of chromatin was used for immunoprecipitation with appropriate antibodies [Phospho-Sat3 (Tyr705) from Cell Signaling (9131; 10ml) and normal rabbit IgG from Vectors laboratories (I-1000; 10mg)] in a total volume of 300ml. After overnight incubation at 4°C, 25μl protein-A Dynabeads (Invitrogen) was added and incubate for more than 1 hour. Beads were

extensively washed and immunoprecipitated complexes were eluted in buffer E (50mM sodium bicarbonate; 1 % SDS). Cross-links were reversed overnight at 65°C. Samples were treated with proteinase K and the DNA was extracted using phenol-chloroform. Quantitative real-time PCR was performed using SYBR Green I (LightCycler 480, Roche). Enrichment for a specific DNA sequence was calculated using the comparative Ct method. The numbers presented with standard errors are based on two biological repeats (cells/chromatin/IP). Primers used in the PCR reactions were analyzed for specificity, linearity range and efficiency in order to accurately evaluate occupancy (percent of IP/input). VEGF primers were used as positive control, while OR8J1 primers were used as negative control.

***Supplemental Tab.1. Patients providing blood (buffy coat) and lung tissue*:**

iPAH: idiopathic PAH; SSC-PAH: PAH associated with scleroderma; SSC: scleroderma; PAH class1: PAH defined as group 1 based on latest World health organization WHO classification.

	Patient type	Sex	Age	Mean PA pressure (mmHg)	PVR (dyne*sec)/cm^5	Buffy Coat	Lung tissue
1	Healthy	F	35	ND	ND	No	Yes
2	Healthy	F	38	ND	ND	No	Yes
3	Healthy	M	45	ND	ND	No	Yes
4	Healthy	M	51	ND	ND	No	Yes
5	Healthy	M	48	ND	ND	No	Yes
6	Healthy	F	44	ND	ND	No	Yes
7	Healthy	F	47	ND	ND	No	Yes
8	Healthy	F	50	ND	ND	No	Yes
9	Healthy	F	30	ND	ND	Yes	No
10	Healthy	F	40	ND	ND	Yes	No
11	Healthy	F	25	ND	ND	Yes	No
12	Healthy	F	27	ND	ND	Yes	No
13	Healthy	M	72	ND	ND	Yes	No
14	Healthy	M	64	ND	ND	Yes	No
15	Healthy	M	18	ND	ND	Yes	No
16	iPAH	M	67	30	219.35	Yes	No
17	iPAH	F	34	62	770.37	Yes	No
18	iPAH	F	24	69	884.21	Yes	No
19	iPAH	F	25	32	279.36	Yes	No
20	iPAH	F	48	29	381.32	Yes	No
21	iPAH	M	57	36	885.71	Yes	No
22	iPAH	F	29	55	1050	Yes	No
23	iPAH	M	68	92	1276.92	Yes	No
24	iPAH	F	58	56	1709	No	Yes
25	iPAH	F	36	67	2274	No	Yes
26	iPAH	F	44	40	755.55	Yes	No
27	SSC-PAH	F	57	56	569.23	Yes	No
28	SSC-PAH	F	59	41	558.49	Yes	No
29	SSC-PAH	F	66	123	1403.07	Yes	No
30	SSC-PAH	F	55	48	980	No	Yes
31	SSC-PAH	F	63	35	546.34	Yes	No
32	PAH group1	F	64	59	926	No	Yes
33	PAH group1	M	72	39	11.7	No	Yes
34	PAH group1	M	58	42	991	No	Yes
35	PAH group1	F	51	51	1199	No	Yes
36	PAH group1	F	48	73	1800	No	Yes
37	PAH group1	F	51	41	990	No	Yes
38	PAH group1	F	68	37	544	No	Yes
39	SSC only	F	63	ND	ND	Yes	No
40	SSC only	F	69	ND	ND	Yes	No
41	SSC only	F	48	22	208.69	Yes	No
42	SSC only	F	46	ND	ND	Yes	No
43	SSC only	F	51	ND	ND	Yes	No
44	SSC only	M	55	28	177.77	Yes	No
45	SSC only	F	64	21	84.21	Yes	No

Supplemental Tab.2: list of all the supplied used with catalog number.

Supply			**Catalog number**
Pim1 Antibody	Cell Signaling		2907 & 3247
Bad Antibody			9292
PS112-Bad Antibody			9291
STAT3 Antibody			9139
PY705-STAT3 Antibody			9131
Akt Antibody			9272
PS473-Akt Antibody			9271
STAT1			9172
PY701-STAT1 Antibody			9171
STAT5 Antibody	SIGMA		S6058
PY694-STAT5 Antibody	Cell Signaling		9351
SM-Actin Antibody	Santa Cruz Biotechnology		M08851
	SIGMA	St Louis, MO, USA	A2547
NFATc2 Antibody	ABCAM		ab2722
FLUO3AM	Invitrogen	Eugene, OR, USA	F1242
TMRM			H1399
Mitotracker Red			M22425
STAT3 Inhibitor Peptide	EMD Bioscience	Mississaga, ON, CANADA	573096
STAT3 Inhibitor Peptide Inactive Control			573105
Quercetagetine			551590
PDGF			521200
TNF-α			654205
Angiotensin II			52-23-0111
Endothelin 1			05-23-3800
Silencer Pim1 Hs	Applied Biosystem	Foster, CA, USA	s10527
Silencer Pim1 Rn			s128205
Silencer STAT3 Hs			s745
SiNegatif			AM4638
18S			431083E
Rn Pim1			284083
Hs Pim1			6581046
Mm Pim1			733876
Hs NFATc2			852882
Rn NFATc2			
Mm NFATc2			787327
Monocrotaline	SIGMA	St Louis, MO, USA	c2401
TUNEL	Millipore		S7110
PCNA	Dako Cytomation	Carpinteria, CA, USA	M0879
Invivofectamine	Invitrogen	Eugene, OR, USA	1377-901

Supplemental Figure 1

A *Pim1 expression is increased in human distal PAs of PAH-patients*

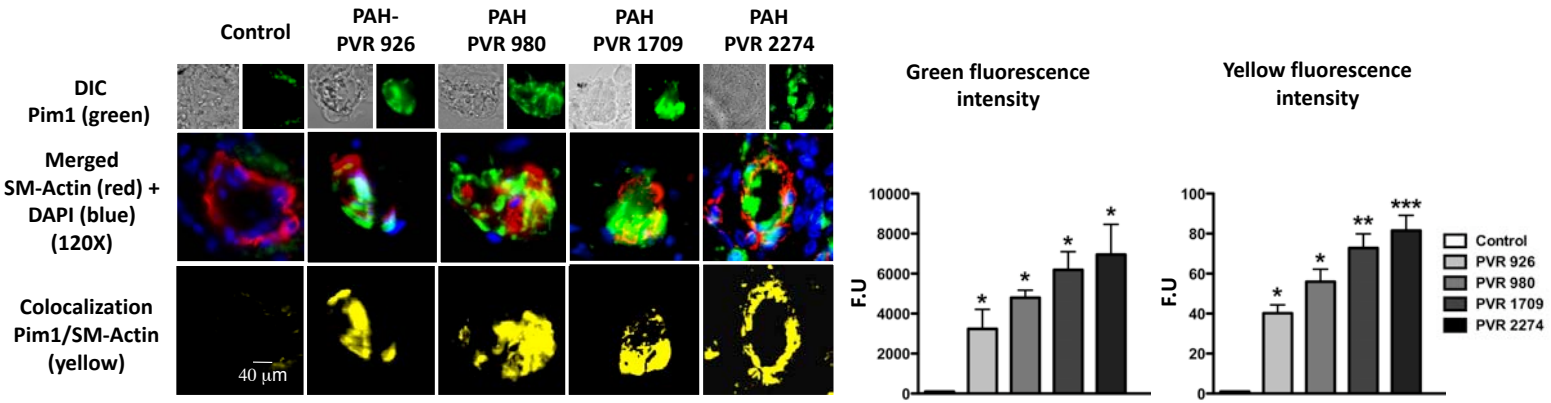

B *Pim1 expression is increased in human white blood cells and correlates with PAH severity*

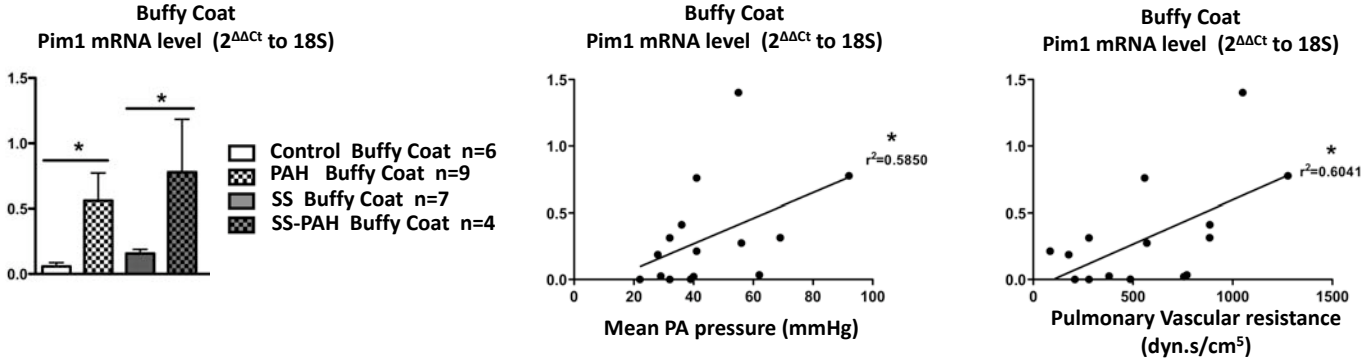

Supplemental Figure 2

A ***Conserved STAT3 binding site in 3' region of Pim1 gene***

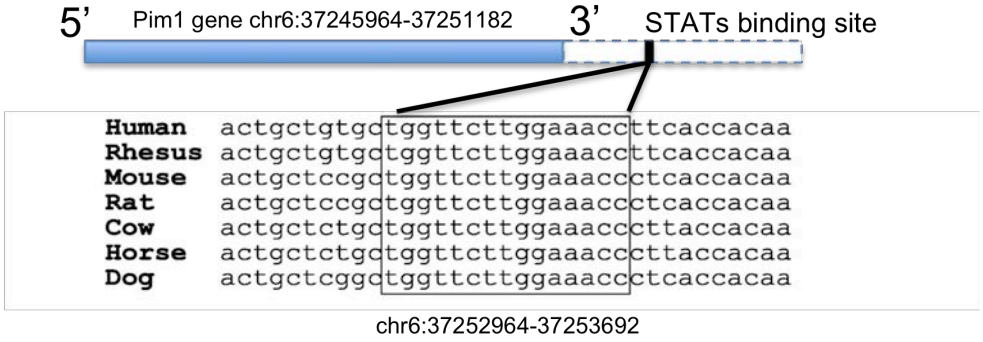

B ***STAT3 binds 3' region of Pim1 gene- ChIP-PCR***

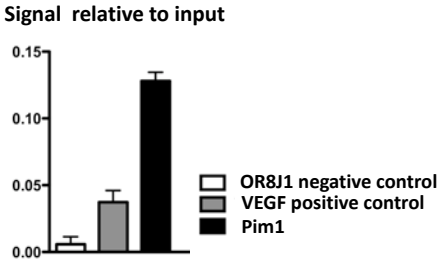

Supplemental Figure 3

A ***STAT1, STAT5 and Akt pathways are not activated in PAH-PASMC***

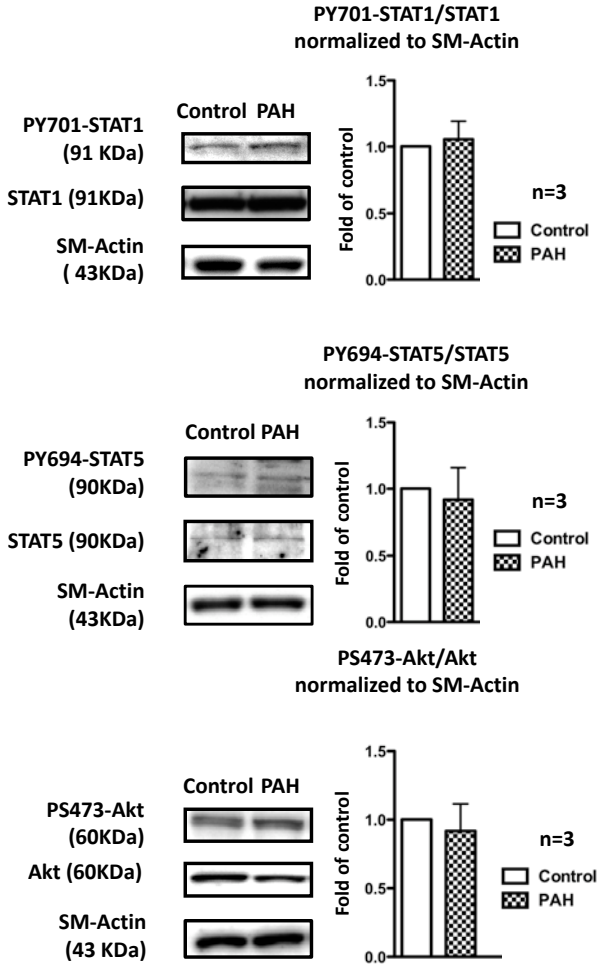

Supplemental Figure 4

A ***Pim1 inhibition reverses PDGF and endothelin-induced proliferation and resistance to apoptosis***

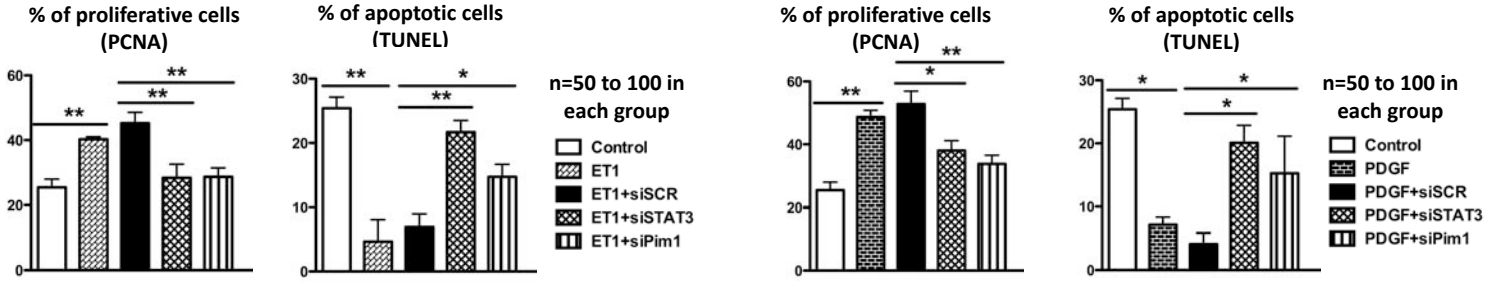

B ***Similarly to Pim1 inhibition, STAT3 inhibition restores mitochondrial functions by depolarizing ΔΨm in PAH-PASMC***

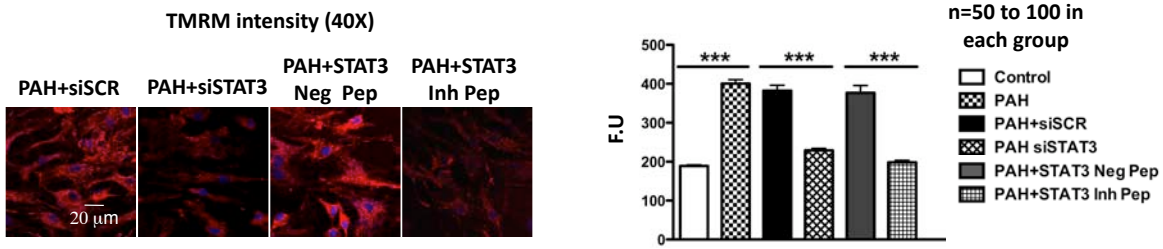

Supplemental Figure 5

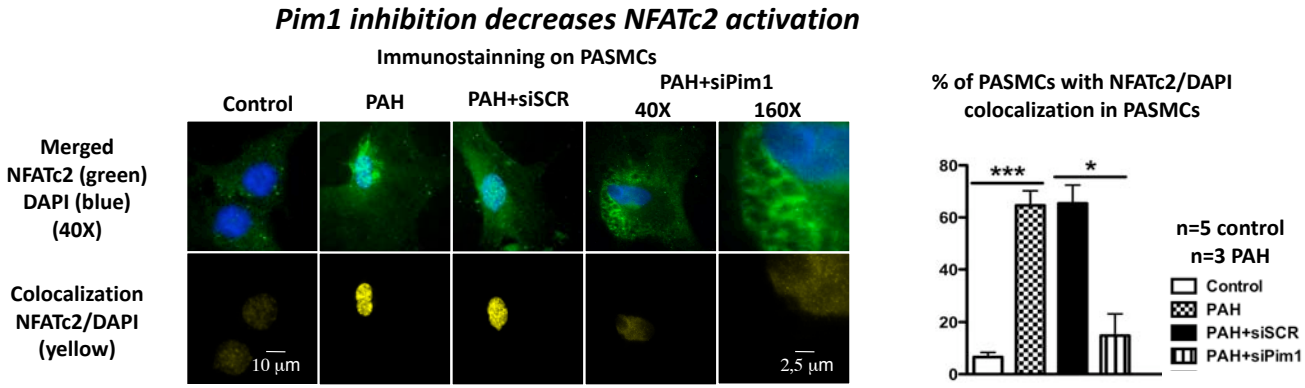

Supplemental Figure 6

A *Pim1 expression increases with PAH development in MCT-PAH rat model.*

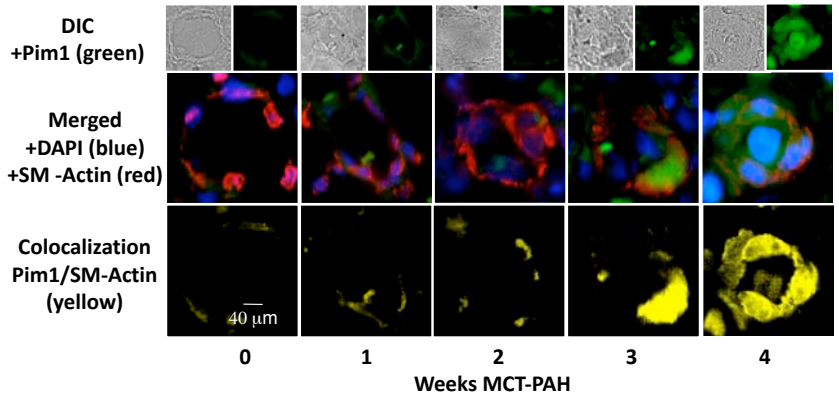

B *Pim1 is not expressed in endothelial cells of PA from MCT-PAH rat model.*

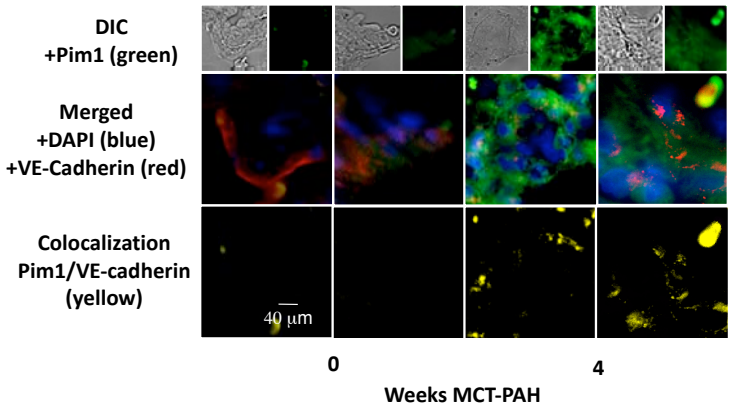

C *STAT3/Pim1/NFATc2 protein expression in MCT-PAH rats lungs*

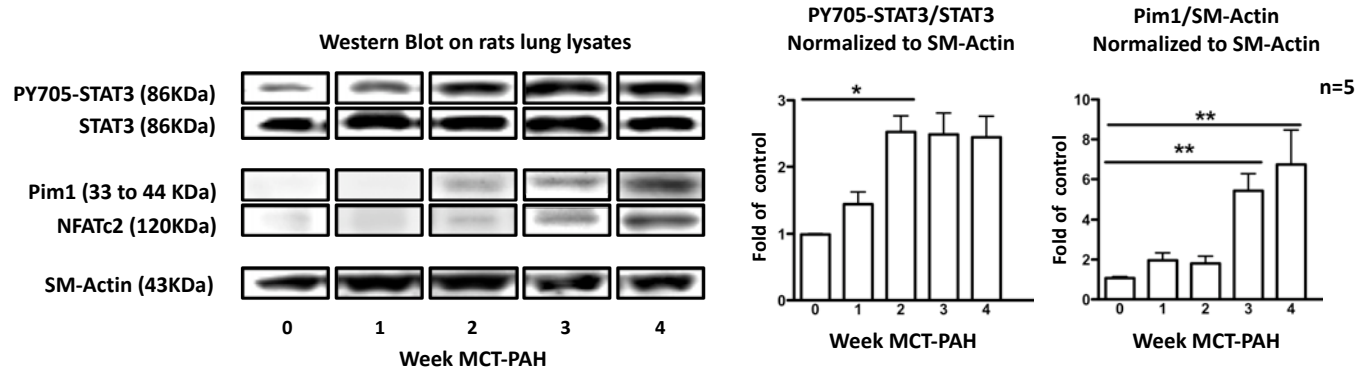

Supplemental Figure 7

A ***Pim1 expression is increased in rats white blood cells and correlates with MCT-PAH severity***

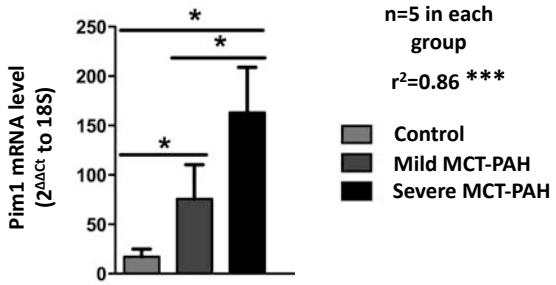

B ***Pim1 mRNA tissue specific expression in MCT-PAH***

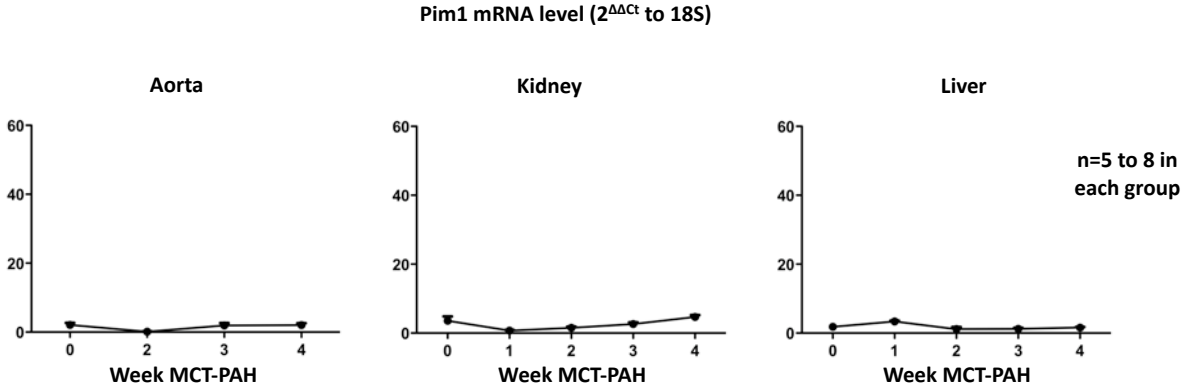

Supplemental Figure 8

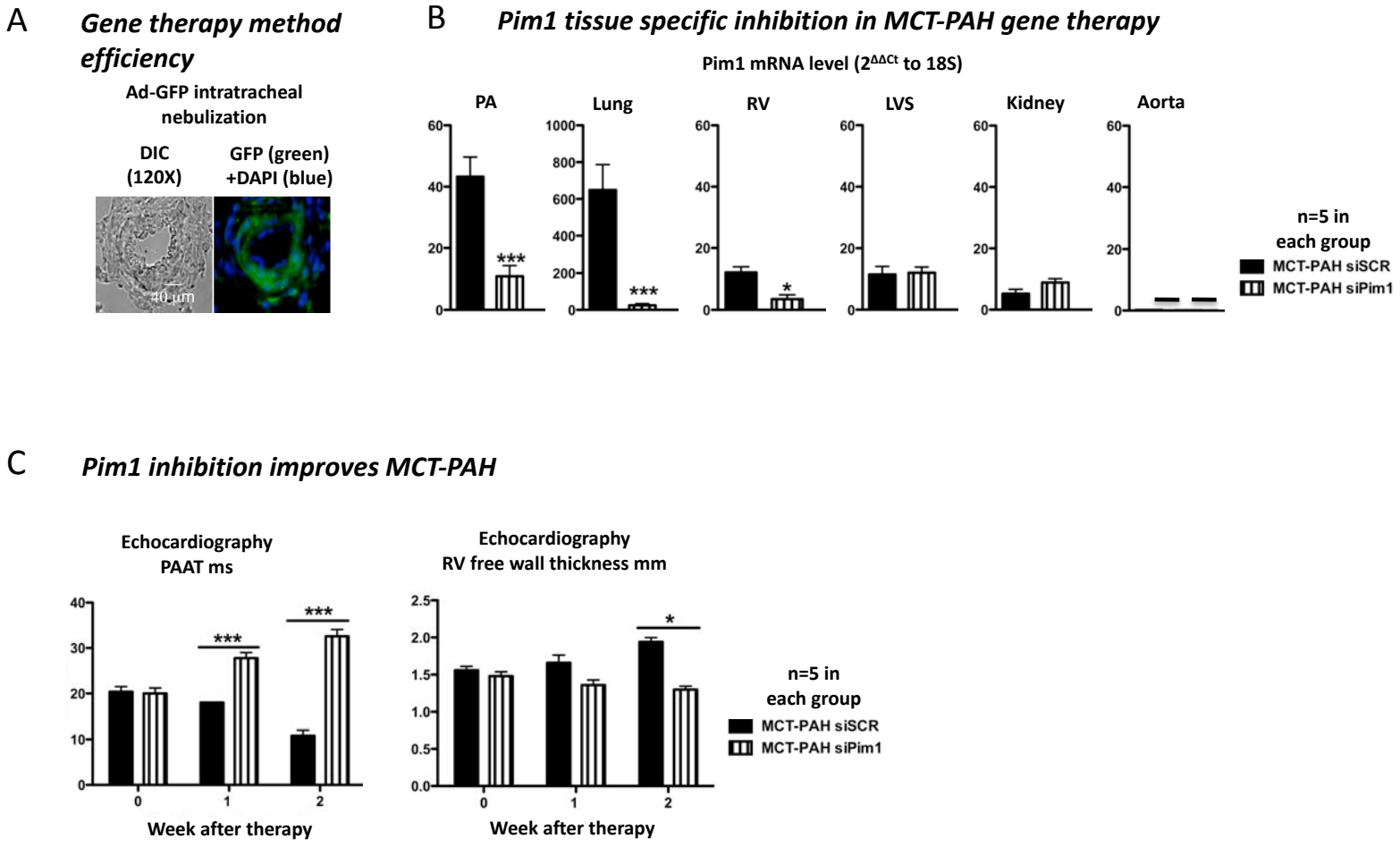

Supplemental Figure 9

A ***Pim1 KO mice are resistant to MCTP and Chronic hypoxia-induced PAH***

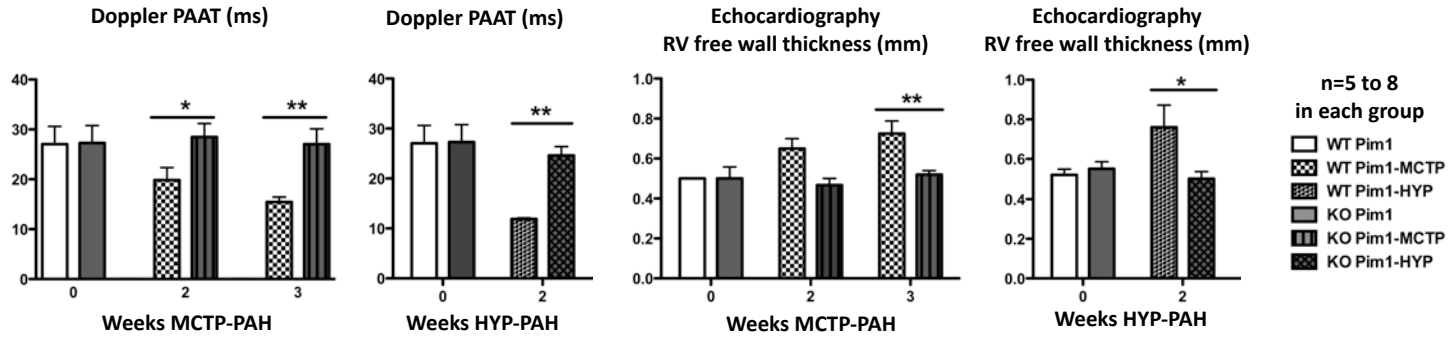

B ***Pim1 KO mice have improved survival***

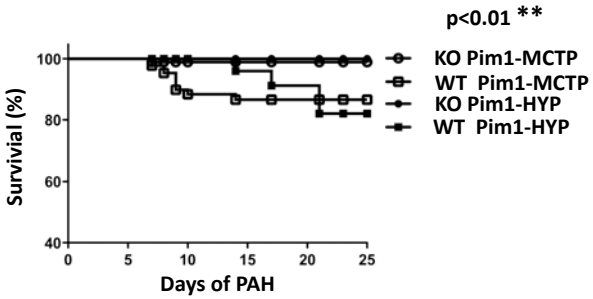

Supplemental Figure 10

A *STAT3 activation in Mice*

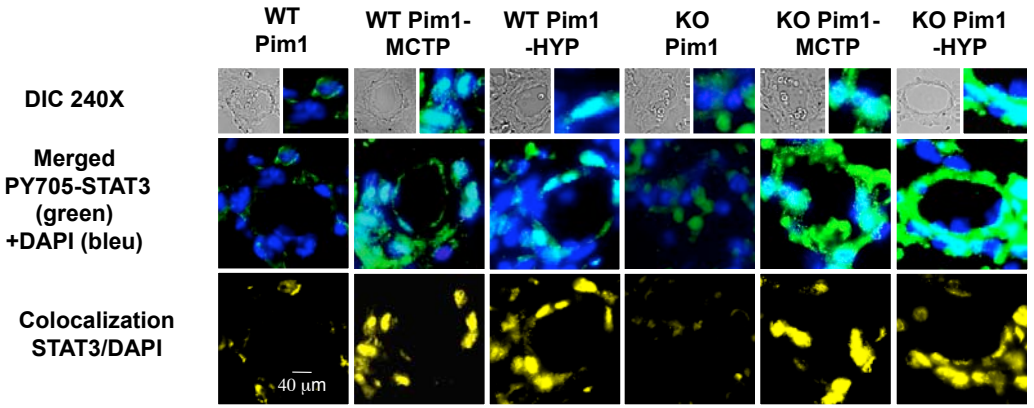

B *NFATc2 activation in Mice*

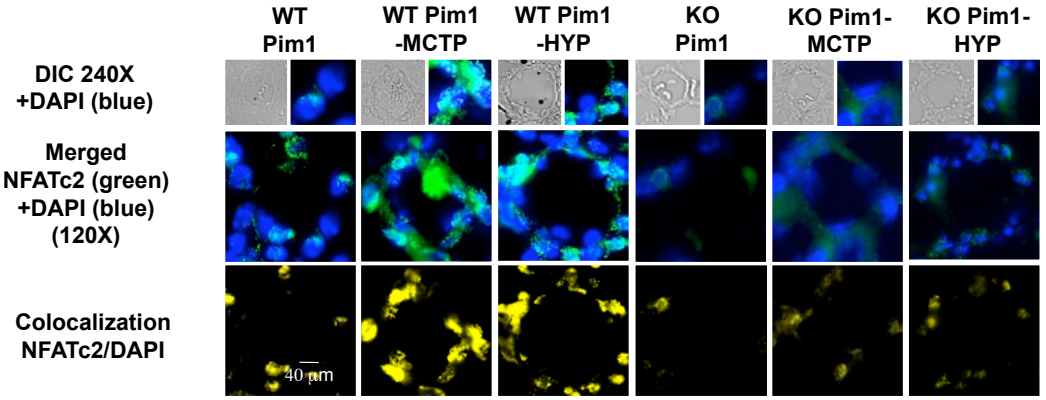

Supplemental Figure 11

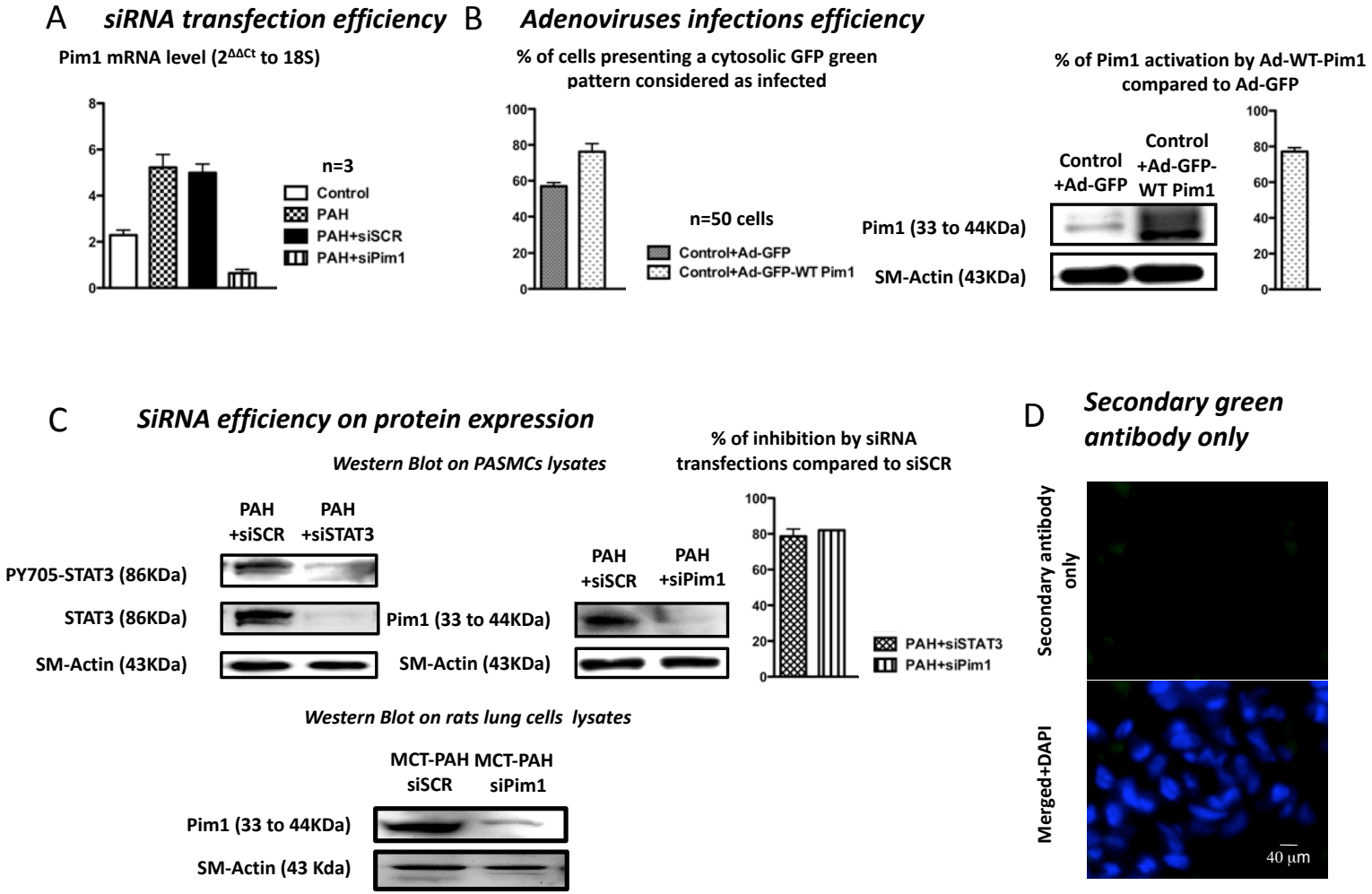

Supplemental Figure Legends

Supplemental Fig.1: **Pim1 expression correlates with PAH severity in humans PAs and buffy coat.**

(A) Pim1 protein expression was measyred by immunofluorescence in human distal PAs of patients with various degrees of PAH (measured by PVR). As shown the greater is the PVR the greater is Pim1 expression (green $p<0.05$). Finally in PAs Pim1 co-localized with SM-actin (red) giving a yellow staining, confirming that Pim1 expression in PAs is mainly localized within PASMCs. As predicted by the amount of Pim1 (green), the amount of yellow was also proportional to PAH severity ($p<0.05$ compared to control group).

(B) Similarly to human PAs, Pim1 mRNA expression is increased in buffy coat of PAH patients and correlates with PAH severity (assessed by PVR and mean PA pressure). We demonstrated that the increase in Pim1 is specific to PAH as patients with scleroderma only showed significantly ($p<0.05$) less Pim1 mRNA compared to both patients with PAH associated or not with scleroderma.

Supplemental Fig.2: **STAT3 binds to the 3' region of Pim1 gene.**

(A) In silico analysis using ENCODE Chip-Seq database confirmed the presence of highly conserved (among several species) STAT binding site in the 3' of Pim1 gene.

(B) STAT3 binding in 3' of Pim1 gene was confirmed in ET-1 stimulated PASMCs by ChIP-PCR (n=3 ChIP/patient in 3 patients). Compared to both VEGF (positive control) and OR8J1 (negative control) STAT3 binding was increased in 3' region of Pim1 gene.

Supplemental Fig.3: **Role of the STAT and Akt pathways in human PAH.**

(A) STAT1 and STAT5, the 2 other STAT isoforms implicated in cardiovascular diseases are not activated in human PAH-PASMC. Immunoblots showed that compare to control-PASMC PY701-STAT1/STAT1 and PY694-STAT5/STAT5 ratios were not significantly changed in PAH-PASMC (n=3 western blot/patients in 3 PAH and 3 control

patients). In addition to the STAT pathway, Akt has been implicated in Pim1 activation. Nonetheless, Akt pathway is not activated in PAH-PASMC (no significant increase in PS473-Akt/Akt ratio).

Supplemental Fig.4: **Role of STAT3/Pim1 in PASMC proliferation and apoptosis**

(A) Pim1 inhibition reverses ET-1 and PDGF induced PASMC proliferation and resistance to apoptosis. ET-1 and PDGF treatment for 48h in control PASMC promotes ($p<0.01$) PASMC proliferation (%PCNA) and resistance ($p<0.01$) to serum starvation induced apoptosis (%TUNEL) as seen in PAH-PASMC. Similarly to STAT3 inhibition (siRNA) Pim1 inhibition reverses this phenotype (n=50 to 100cells/patient in 5 control patients; $p<0.05$).

(B) STAT3 inhibition by either siRNAs or inhibitor peptide restores mitochondrial membrane potential measured by TMRM ($p<0.05$; n=50 to 100cells/patient in 3 PAH patients) in PAH-PASMCs.

Supplemental Fig.5: **Pim1 inhibition decreases NFATc2 activation in PAH-PASMCs.**

(A) Pim1 inhibition using siRNAs decreases NFATc2 (green) nuclear translocation (DAPI blue) giving less yellow staining, in 10 to 20 cells /patient in 3 PAH and 5 control patients.

Supplemental Fig.6: **Pim1 expression is increase in MCT-induced PAH in rat and is confined to the PASMCs.**

(A) Pim1 expression was measured by immunofluorescence in distal PAs in lungs biopsies of both control and MCT-injected rats. Pim1 expression (green) increases with the development of PAH (i.e there is an increase in Pim1 expression (more green fluorescence) two weeks post MCT injection). Moreover, colocalization experiments between SM-Actin (red) and Pim1 (green) showed that the increased in Pim1 expression in mostly confined to PASMCs giving a greater yellow staining 2 weeks and beyond MCT-injection.

(B) Double staining technique with VE-cadherin a marker of endothelial cells, showed limited co-localization between Pim1 (green) and VE-cadherin (red), suggesting that Pim1 is primarily expressed in PASMCs and less in PA endothelial cells.

(C) As in human, the increase in Pim1 expression is precede by a significant activation of STAT3 ($p<0.05$) (measured by the P-STAT3/STAT3 ratio using immunoblots) between 1 and 2 weeks post MCT injection. Similarly, NFATc2 protein expression follows the same expression pattern than Pim1.

Supplemental Fig.7: **(A) Pim1 expression is increased in rats white blood cells and correlates with MCT-PAH severity.** Pim1 mRNA levels were measured in buffy coat from control rats (mean PAP <15mmHg); and rats with MCT-induced mild-PAH (mean PAP <30mmHg) and sever PAH (mean PAP greater than 30mmHg). As shown, Pim1 mRNA levels are significantly increase in both mild and sever-PAH rats compare to control. In addition a significant correlation was found between Pim1 mRNA levels and PAH severity (n=5 to 8 rats per group). **(B) Pim1 expression in various tissues.** Pim1 mRNA levels were measured in several tissues including aorta; kidney and liver by qRT-PCR. As shown, Pim1 is poorly expressed at mRNA level in the tested tissues, and is not affected by development of PAH.

Supplemental Fig.8: **Pim1 inhibition affects only the pulmonary arteries reversing PAH.**

(A) To verify the tissue distribution of our treatment we also nebulized an adenovirus carrying GFP. We observed the expression of GFP using immunofluorescence staining on lung sections. Diffuse GFP immunofluorescence in the PAs confirmed the tissue specificity of our nebulization technique. This experiment doesn't show that our method of silencing is effective but allows verifying the instrumentation and that nebulization occurred.

(B) In order to study the selectivity and safety of our gene silencing delivery method, we measured Pim1 expression in several tissues. We showed that siRNA treated rats had decreased Pim1 mRNA levels in lung, PAs and RV but not in other systemic vessels such as aorta, while

rats treated with scrambled siRNA showed no modification in Pim1 levels. Note that Pim1 levels were very low in all other tested organs and their levels were similar in the siRNA and scrambled treated rats showing the tissue specificity of our therapeutic intervention.

(C) Longitudinal studies using echography and Doppler showed that Pim1 inhibition significantly increases PAAT ($p<0,001$) and decreases RV hypertrophy ($p<0,05$).

Supplemental Fig.9: **Pim1 K.O mice are resistant to PAH.**

(A) Longitudinal studies using echocardiography and Doppler showed that Pim1 K.O mice are resistant to both MCTP and chronic hypoxia induced PAH, as no changes in PAAT and RV hypertrophy were observed, while like in rats wild type mice injected with MCTP or exposed to CH had a significant ($p<0.05$) decrease in PAAT and significant increase in RVH.

(B) Pim1 K.O mice have improved survival over 25 days period post MCTP injection or CH exposure ($p<0.01$).

Supplemental Fig.10: **STAT3 and NFATc2 activation in Pim1 K.O.**

(A) As in rats STAT3 activation (PY705-STAT3 in green nuclear translocation) is increased in both WT and Pim1 KO mice injected with MCTP or exposed to chronic hypoxia giving a greater yellow staining.

(B). NFATc2 activation measure by NFATc2 (green) nuclear translocation, is increased only in WT animals injected with MCT or exposed to CH (increased yellow staining). As predicted lack of Pim1 in KO animals prevented NFATc2 activation. This finding suggests that STAT3 activation is not sufficient to activate NFAT and to promote PAH.

Supplemental Fig.11: **Efficiency of Pim1 siRNA, adenoviruses, STAT3 siRNA and antibody immunofluorescence specificity.**

(A) Using qRT-PCR we demonstrated that our concentration of Pim1 siRNAs block over 80% of Pim1 mPNA expression in PAH-PASMCs, while the same concentration of scrambled siRNA has no effect.

(**B**) Adenoviruses infection at 1.10^7 PFU induce an infection rate of 60 to 80% in healthy PASMCs exposed to 48h. Wild type Pim1 adenovirus infection in healthy-PASMC promotes Pim1 expression by 80%.

(**C**) Immunoblots performed in human PAH-PASMCs showed that both siSTAT3 and siPim1 blocks 80% of STAT3 and Pim1 the protein expression respectively. Similar results were found in the lungs of MCT-PAH rats nebulized with siPim1.

(D) Staining with only the same secondary antibody (green signal) used for Pim1, NFATc2 and Bcl2 immunofluorescence showed no unspecific staining in human distal PA.

Supplemental References

1. Bonnet S, Archer SL, Allalunis-Turner J, Haromy A, Beaulieu C, Thompson R, Lee CT, Lopaschuk GD, Puttagunta L, Bonnet S, Harry G, Hashimoto K, Porter CJ, Andrade MA, Thebaud B, Michelakis ED. A mitochondria-K+ channel axis is suppressed in cancer and its normalization promotes apoptosis and inhibits cancer growth. Cancer Cell. 2007; 11:37-51.

2. McMurtry MS, Archer SL, Altieri DC, Bonnet S, Haromy A, Harry G, Bonnet S, Puttagunta L, Michelakis ED. Gene therapy targeting survivin selectively induces pulmonary vascular apoptosis and reverses pulmonary arterial hypertension. J Clin Invest. 2005; 115:1479-1491.

3. Bonnet S, Paulin R, Sutendra G, Dromparis P, Roy M, Watson KO, Nagendran J, Haromy A, Dyck JR, Michelakis ED. Dehydroepiandrosterone reverses systemic vascular remodeling through the inhibition of the Akt/GSK3-{beta}/NFAT axis. Circulation. 2009; 120:1231-1240.

4. Bonnet S, Rochefort G, Sutendra G, Archer SL, Haromy A, Webster L, Hashimoto K, Bonnet SN, Michelakis ED. The nuclear factor of activated T cells in pulmonary arterial hypertension can be therapeutically targeted. Proc Natl Acad Sci U S A. 2007; 104:11418-11423.

5. Raoul W, Wagner-Ballon O, Saber G, Hulin A, Marcos E, Giraudier S, Vainchenker W, Adnot S, Eddahibi S, Maitre B. Effects of bone marrow-derived cells on monocrotaline- and hypoxia-induced pulmonary hypertension in mice. Respir Res. 2007; 8:8.

6. Mattocks AR, Jukes R, Brown J. Simple procedures for preparing putative toxic metabolites of pyrrolizidine alkaloids. Toxicon. 1989; 27:561-567.

7. Sutendra G, Bonnet S, Rochefort G, Haromy A, Folmes KD, Lopaschuk GD, Dyck JR, Michelakis ED. Fatty acid oxidation and malonyl-CoA decarboxylase in the vascular remodeling of pulmonary hypertension. Sci Transl Med. 2010; 2:44-58.